

# Contaminant characteristics and environmental risk assessment of heavy metals in the paddy soils from lead (Pb)-zinc (Zn) mining areas in Guangdong Province, South China

Da-Mao Xu<sup>1,2,3</sup> · Bo Yan<sup>1,2</sup> · Tao Chen<sup>1,2</sup> · Chang Lei<sup>1,2</sup> · Han-Zhi Lin<sup>1,2,3</sup> · Xian-Ming Xiao<sup>1,2</sup>

Received: 15 June 2017 / Accepted: 29 August 2017 / Published online: 10 September 2017  
© Springer-Verlag GmbH Germany 2017

**Abstract** In November 2016, the total metal concentrations in nine representative locations in lead (Pb)-zinc (Zn) mining areas, located in Guangdong Province, South China, were determined experimentally by flame atomic absorption spectrometer. The results indicated that the paddy soils were heavily contaminated with Cd ( $20.25 \text{ mg kg}^{-1}$ ), Pb ( $1093.03 \text{ mg kg}^{-1}$ ), and Zn ( $867.0 \text{ mg kg}^{-1}$ ), exceeding their corresponding soil quality standard values and background values. According to the results, the mean enrichment factor levels of the studied metals decreased in the following order: Cd > Zn > Pb > Cu > Ni > Mn > Cr. Among these metals, Cd, Pb, and Zn were predominantly influenced by widespread anthropogenic activities. The highest concentrations of the studied metal pollutants were distributed in the areas surrounding the mining activity district. Multivariate statistical analysis indicated that the major contributing sources of the studied metals were metal ore mining, smelting, and processing activities. However, the composition of soil background was another potential source. Moreover, the assessment results of environment risks showed that the potential ecological

risks, in decreasing order, were Cd > Pb > Zn > Cu > Ni > Cr > Mn. Additionally, the non-carcinogenic risk represented the trend of  $HI_{Pb} > HI_{Mn} > HI_{Zn} > HI_{Cu}$ , and the carcinogenic risk ranked as  $CR_{Cr} > CR_{Cd} > CR_{Ni}$ . Among the environmental risk substances, Cd and Pb were the main contributors that pose ecological harm and health hazards through their serious pollution. Consequently, greater attention should be paid to this situation.

**Keywords** Lead-zinc mining area · Paddy soils · Heavy metals · Contaminant characteristics · Environmental risk assessment

## Introduction

Soil contamination by heavy metals with increasing environmental consequences has received global attention (Gąsiorek et al. 2017; Liang et al. 2017; Ran et al. 2017). Various anthropogenic activities have progressively exacerbated the prevalence and occurrence of soil contamination with heavy metals over decades (Ungureanu et al. 2016). As is well known, lead and zinc occur naturally in sulfide mineral ores, and excessive excavation of these ores has caused re-release of these heavy metals generally bonded to sulfide minerals, resulting in soil acidification. Additionally, long-term mining and smelting operations have caused discharge of huge untreated tailing ponds and mining wastes that are then exposed to natural mechanisms, such as rain runoff and weathering processes. These processes in turn generate acid mine drainage (AMD) contaminated with large quantities of heavy metals (Liao et al. 2017; Liao et al. 2016), which is regarded as one of the most influential anthropogenic activities (Li et al. 2014). Even worse, mineral mining activities have translocated significant amounts of heavy metals into agricultural soils (Obiora et al. 2016).

Responsible editor: Zhihong Xu

✉ Bo Yan  
yanbo2007@gig.ac.cn

<sup>1</sup> State Key Laboratory of Organic Geochemistry, Guangzhou Institute of Geochemistry, Chinese Academy of Sciences, Guangzhou 510640, People's Republic of China

<sup>2</sup> Guangdong Key Laboratory of Environmental Protection and Resources Utilization, Guangzhou Institute of Geochemistry, Chinese Academy of Sciences, Guangzhou 510640, People's Republic of China

<sup>3</sup> University of Chinese Academy of Sciences, Beijing 100082, People's Republic of China

Once the heavy metals are accumulated excessively in soils, they can undesirably affect the physicochemical properties and functions and obstruct the nutrient supply in soils (Liang et al. 2017; Zhang et al. 2016; Zhao et al. 2014). Subsequently, heavy metal contents negatively cause decreases in soil fertility, degeneration of the ecosystem, and reduction in crop productivity. These metals can also exert their potentially toxic and carcinogenic effects when finding their ways into agricultural products and human bodies and thus ultimately pose environmental risks to both ecological security and human well-being (Lei et al. 2016). Due to the facts noted above, environmental sampling of soils has become the most effective and sensitive indicator to estimate anthropogenic contamination by heavy metals.

A state-owned lead-zinc mine, located in the northern region of Guangdong Province, South China, is a representative and important producing zone of large-scale metallic symbiotic mineralization (Fig. 1), with a nearly 50-year exploitation history and still large reserves of lead and zinc. Metalliferous industries are a double-edged sword. While the local socio-economic development benefits from the historical mining activity, simultaneously, the adjoining environments in the vicinity of mining districts are seriously contaminated by heavy metals. Worse still, hazardous metals have a higher tendency to accumulate continuously in soils around mining and smelting areas. Unfortunately, information on the undesirable impacts of the mining operations on the ecology and human health is still very rare. Hence, it is important to estimate qualitatively the growing environmental risk of soils contaminated with heavy metals derived from metal-mining operations (Lei et al. 2016; Ungureanu et al. 2016). For this reason, numerous studies on the pollution assessment, source identification, chemical fractions, and pattern distribution of

heavy metals in mine-impacted soils have been extensively reported (Dehghani et al. 2016; Fernández-Calviño et al. 2017; Kpan et al. 2014; Rajaei et al. 2015). Nevertheless, there has been relatively little focus on a multimetal assessment of environmental pollution risks based on the potential ecological risk index (PERI) method and health risk assessment (HRA) model in conjunction with multivariate statistical analysis.

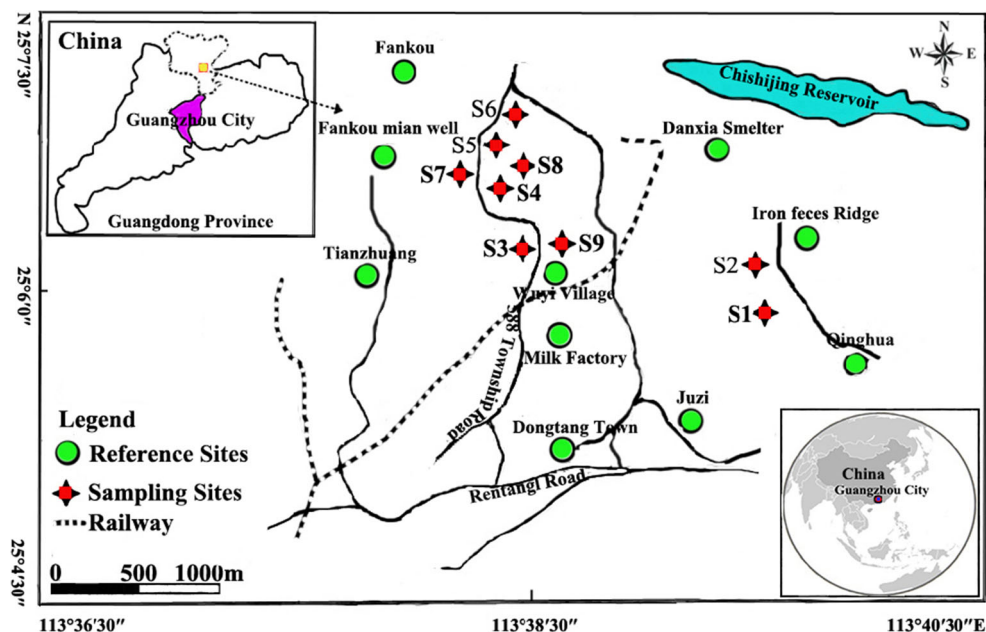
Accordingly, the overall purposes of the current study were as follows: (a) to investigate and compare the accumulation levels of heavy metals in paddy soils, (b) to better address the spatial characteristics of heavy metal concentration, (c) to determine the likely sources of the heavy metals in combination with multivariate statistical analysis, and (d) to quantitatively evaluate the potential ecological and health risks of the seven essential heavy metals that were considered because of their accumulative behaviors and non-biodegradability to ascertain whether heavy metal-rich pollution is safe for ecosystems and sensitive populations or not. Locally, the comprehensive information can contribute to providing priority-based schedules for innovative pollution prevention and environmental risk management in industrial cities.

## Materials and methods

### Description of study area

A comprehensive field survey to acquire adequate information about conditions surrounding the lead-zinc mines was conducted by our research group previously. According to the local land use map, the study area is situated between 113° 37' 30" and 113° 40' 30" east longitude and 25° 6' 0" and 25°

**Fig. 1** Map of the study area showing sampling sites



7' 30" north latitude, selected from the concentrated contiguous rice fields between the ore digging and smelting sites as described in Fig. 1. Simultaneously, the localized residential setting (Wuyi village) was also taken into account, where the local inhabitants are unaware of the adverse health effects posed directly by mining pollution. In this region, soil enrichment by heavy metals was correlated with the effluent-producing mining industry. In addition, potential secondary sources are the local intense agricultural production, industrial practices, and very high-traffic activities.

### Collection of soil samples

In November 2016, a randomized sampling method was used to establish the sampling network near a typical lead-zinc mine (Fig. 1), modified from the Technical Specification for Soil Environmental Monitoring (HJ/T 166-2004). Each topsoil (0–20 cm) sample with a total weight of approximately 1.5 kg was obtained separately from nine representative sampling sites using a wooden shovel after rice was harvested. A total of five to six subsamples were taken within an area of  $2 \times 2$  m in each representative sample and were then combined in the field as an individual composite sample. The geographical coordinates were recorded in detail for these sampling sites with the help of a Geographical Position System (GPS) device. All collected samples were packed into labeled polythene bags, sealed tightly, and quickly transported to laboratories for further processing.

### Preparation, processing, and analyses of soil samples

The collected samples were air dried for 1 week at room temperature. All samples were passed through a 100-mesh sieve after pretreatment operations that included crushing, removal of unwanted impurities completely (stones, roots, grit, plant debris, etc.), and pulverization to a fine powder. The soil powders were stored in clean polyethylene bags for further content analysis. Upon analysis, approximately 0.5000 g of each homogenized powder sample was weighed accurately, placed in a Teflon digestion crucible on an electro-thermal board, moistened with 1 mL distilled water, and digested with a 9:3:6:2 mixture ratio of HCl-HNO<sub>3</sub>-HF-HClO<sub>4</sub> in a three-step process at different constant temperatures for approximately 24 h. Before being allowed to nearly evaporate to dryness with no more white fuming, the extracted solutions were decanted into glass tubes after cooling, subsequently diluted to 50 mL with 2% ultrapure HNO<sub>3</sub>, and later filtered off using 0.45- $\mu$ m membrane filters before analysis. Afterward, the total contents of chromium (Cr), nickel (Ni), cadmium (Cd), copper (Cu), lead (Pb), zinc (Zn), and manganese (Mn) in the digested solutions were quantitatively determined by an atomic absorption spectrometer (AAS, Hitachi ZA3000, Japan).

### Quality control and statistical analysis

All reagents procured were of analytical grade unless otherwise specified. Prior to analysis, all the glassware and the Teflon crucibles used in the study were soaked overnight with 20% HNO<sub>3</sub> and then rinsed thoroughly with deionized water to prevent external contamination. To evaluate residual effects related to the previous sample analysis, a 10-s washing occurred between two subsequent samples. Calibration curves constructed by the regression calibration method were linear with a correlation coefficient ( $r^2$ ) greater than 0.9990 for the studied metals. Each sample was prepared in three analytical replicates, and relative standard deviations (RSDs) of the three analytical results were calculated and were found to be less than 10%. Analytical blanks were routinely run in the same procedure as the samples and were used to correct all analytical data. To ensure the analytical precision and accuracy, the certified concentrations of reference materials (GSS-16 and GSD-6, purchased from the China National Center for Standard Materials) were found to be within the range of acceptable values, and the recoveries varied between 84.26 and 109.10%.

The analytical data were treated and analyzed using Microsoft Excel 2013 and IBM SPSS Statistics 22.0. Additionally, the graphs were analyzed and processed by Origin 9.0 and Adobe Photoshop CS6 software.

### Enrichment factor

In general, the enrichment factor (EF) could be a diagnostic tool to differentiate whether the metals originated from heterogeneous anthropogenic sources or from natural provenance (Dehghani et al. 2016). The EF method was universally defined as presented in the following equation (Jiang et al. 2017; Lin et al., 2017):

$$EF = (X_i/R_n)_{\text{Sample}} / (X_i/R_n)_{\text{Background}} \quad (1)$$

where  $EF$  is the enrichment factor,  $(X_i/R_n)_{\text{Sample}}$  is the concentration ratio of the metal in the tested sample to the reference element, and  $(X_i/R_n)_{\text{Background}}$  is the corresponding reference ratio in the background sample. For  $EF$  calculations, iron (Fe) commonly serves as the conservative reference element to normalize the metal concentrations because it is characterized by relatively higher natural components and stability in the crust (Jiang et al. 2017). In the present study, the background values for the metals previously studied from Guangdong Province soils were adopted as a reference baseline (CNEMC 1990). Five descriptive categories are interpreted based on the  $EF$ , as suggested by Sutherland, in Fig. 2 (Sutherland 2000).

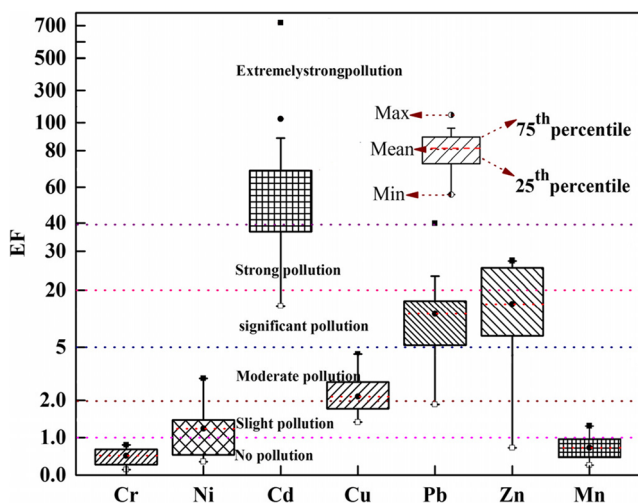


**Fig. 2** Whisker-box plots for enrichment factors ( $EF_s$ ) and pollutant grades of the studied metals in soils

**Potential ecological risk assessment**

Numerous standard indices are often computed to determine the status and degree of heavy metals in soil, including the single-factor pollution index, Nemerow synthesis index, pollution load index, geoaccumulation index, enrichment factor, and potential ecological risk index (Diami et al. 2016; Pan et al. 2016a). However, compared with other methods, the potential ecological risk index (PERI) method has been used widely by many other authors to quantitatively assess the comprehensive potential ecological risks and environmental impacts produced by toxic metals (Diami et al. 2016; Pan et al. 2016a; Wu et al. 2016). The PERI method, originally developed by the Swedish scientist Hakanson (1980) from the sedimentological perspective, offers the advantages of covering various research domains in environmental geochemistry, biological toxicology, and ecological environment (Hakanson 1980). Aside from this, the enrichment level of heavy metals in soil was incorporated to calculate more accurately an appraisal of their potential ecological risks. According to the modified approach (Diami et al. 2016; Hakanson 1980; Pan et al. 2016a; Wu et al. 2016):

$$RI = \sum E_i^r = \sum T_i^r \times EF_i^r \tag{2}$$

where  $RI$  is calculated as the integrated potential ecological risk index for multiple metals, which represents the sensitivity of various biological communities to harmful elements and assesses the degree of heavy metal pollution;  $E_i^r$  represents the potential ecological risk factor;  $T_i^r$  is the toxic response factor for a given substance; and  $EF_i^r$  is the enrichment factor of the heavy metal. Based on Hakanson’s approach, the values of  $T_i^r$  for the heavy metals (Cr, Ni, Cd, Cu, Pb, Zn, and Mn) were determined to be 2, 5, 30, 5, 5, 1, and 1, respectively

(Hakanson 1980). The evaluated criteria on the basis of  $E_i^r$  and  $RI$  calculations are given in Fig. 6.

**Health risk assessment**

The human health risk assessment (HRA) model proposed by the United States Environment Protection Agency (US EPA) was used to estimate the health effects, consisting of carcinogenic and non-carcinogenic risk assessments for heavy metals (US EPA 1989; US EPA 2002; RAIS 2014). According to the International Agency for Research on Cancer (IARC) and Integrated Risk Information System (IAIS), Cu, Pb, Zn, and Mn were identified as non-carcinogenic elements, whereas Cr, Ni, and Cd were classified as potentially carcinogenic elements. In addition, children and adults may be exposed to carcinogenic elements, which are considered only through the inhalation pathway because carcinogenic slope factors are not available for Cu, Pb, Zn, and Mn. Exposure assessment is one of four key steps in the risk assessment procedures (Jiang et al. 2017). For this study, exposure assessment of the local adults and children was carried out by measuring the chronic daily intake ( $ADD$ ) of heavy metal-laden soils earlier identified through multiple pathways (inhalation, ingestion, dermal contact). The corresponding  $ADD_s$  ( $\text{mg kg}^{-1} \text{day}^{-1}$ ) received through the three preferential pathways were separately determined and expressed using the following Eqs. (3)–(5) as separately prescribed by (Diami et al. 2016; Jiang et al. 2017; Pan et al. 2016a; Xiao et al. 2015):

$$ADD_{ing} = \frac{C \times \text{Ingr} \times EF \times ED}{BW \times AT} \times 10^{-6} \tag{3}$$

$$ADD_{inh} = \frac{C \times \text{Inh} \times EF \times ED}{PEF \times BW \times AT} \tag{4}$$

$$ADD_{derm} = \frac{C \times SA \times SAF \times ABS_d \times EF \times ED}{BW \times AT} \times 10^{-6} \tag{5}$$

where  $ADD_{ing}$ ,  $ADD_{inh}$ , and  $ADD_{dermal}$  are the daily exposure doses ( $\text{mg kg}^{-1} \text{day}^{-1}$ ) of soil via the ingestion, inhalation, and dermal contact pathways, respectively.  $C_{UCL95\%}$  ( $\text{mg kg}^{-1}$ ) was calculated as the upper limit of the 95% confidence (95%UCL) interval for the mean, which is considered to yield an estimate of the “reasonable maximum exposure.” With respect to the behavioral and physiological differences that may lead to the uncertainties in the calculations of the  $ADD_s$ , the details of the parameters and their values were preferentially derived from the published studies in China as summarized in Table 1 (MEPPRC 2014; Jiang et al. 2017; Lin et al., 2017; Xiao et al. 2015). Among the China-specific parameters,  $SA$  was achieved by executing the following equation (MEPPRC 2014):  $SA = 239 \times H^{0.417} \times BW^{0.517} \times SER$ .

**Table 1** Parameter values used in the exposure assessment equations

Parameters	Description	Unit	Value	
			Child	Adult
C	Concentration of heavy metal	mg kg <sup>-1</sup>	95%UCL	95%UCL
ED	Exposure duration	a	6	24
BW	Body weight	kg	15.9	56.8
EF	Exposure frequency	days a <sup>-1</sup>	350	
AT	Time for non-carcinogenic effects	days	2190	
	Time for carcinogenic effects	days	26,280	
IngR	Ingestion rate	mg day <sup>-1</sup>	200	100
SAF	The adherence factor	mg (cm <sup>2</sup> day <sup>-1</sup> )	0.2	0.7
SA	Skin surface area	cm <sup>2</sup> day <sup>-1</sup>	2447.6	5074.9
H	Height	cm	99.4	156.3
SER	The ratio of exposed skin area		0.36	0.32
ABS <sub>d</sub>	The dermal absorption factor		0.001	
InhR	Inhalation rate	m <sup>3</sup> d <sup>-1</sup>	7.5	14.5
PEF	Particulate emission factor	m <sup>3</sup> kg <sup>-1</sup>	1.32 × 10 <sup>9</sup>	

For the risk characterization quantified by carcinogenic and non-carcinogenic risk, the total cancer risk ( $CR_n$ ), obtained by summing the individual cancer risks ( $CR_s$ ), was assessed using Eq. (6). The hazard index ( $HI$ ) was calculated to assess the cumulative non-carcinogenic risk generated by each heavy metal from multiple exposure pathways, as expressed in Eq. (7). Similarly, the total hazard index ( $HI_n$ ) was determined by adding the  $HI_s$ , as described by Eq. (8).

$$Cancer\ Risk_n(CR_n) = \sum Cancer\ Risk_{inh}(CR_{inh}) = \sum ADD_{inh} \times SF_{inh} \quad (6)$$

$$HI = \sum (HQ_{ing} + HQ_{inh} + HQ_{derm}) = \sum \left( \frac{ADD_{ing}}{RfD_{ing}} + \frac{ADD_{inh}}{RfD_{inh}} + \frac{ADD_{derm}}{RfD_{derm}} \right) \quad (7)$$

$$Hazard\ Index_n(HI_n) = \sum Hazard\ Index_i(HI_i) \quad (8)$$

where  $SF$  (kg day<sup>-1</sup> mg<sup>-1</sup>) is the carcinogenicity slope factor with exposure to the potentially carcinogenic elements. The reference dose ( $RfD$ ) (mg kg<sup>-1</sup> day<sup>-1</sup>) is the estimated maximum permissible risk to sensitive populations through daily exposure;  $CR_n$  is the multimetals from the inhalation exposure pathway and corresponds to the summation of the cancer risks ( $CR_s$ );  $CR$  estimates the

incremental probability of an individual developing any type of excess cancer over a lifetime as a result of exposure to the potential carcinogenic hazards; and  $HI$  refers to the summation of  $HQ_s$  of each exposure pathway and represents the magnitude of the non-carcinogenic effects from multiple pathways. The  $CDI_{inh}$  is multiplied by the corresponding slope factor ( $SF_{inh}$ ) to yield an estimate of the carcinogenic risks ( $CR_s$ ) (Ferreira-Baptista and Miguel 2005), whereas the hazard quotient ( $HQ$ ) is calculated by dividing the  $CDI$  by a specific  $RfD$  for each metal and exposure pathway (Jiang et al. 2017). Based on review of works widely reported in the literature, the corresponding reference doses ( $RfD_i$ ) and cancer slope factor ( $SF$ ) values are tabulated in Table 2 (Lin et al., 2017; Xiao et al. 2015).

## Results and discussion

### Heavy metal concentrations

The descriptive statistics for the measured metals in the paddy soil samples from the lead-zinc mine areas are summarized in Table 3, which also includes the Chinese soil quality standards and the background values in Chinese soils to facilitate the evaluation and comparison.

**Table 2** The references dose (mg kg<sup>-1</sup> day<sup>-1</sup>) for non-carcinogenic metals and the slope factors (kg day<sup>-1</sup> mg<sup>-1</sup>) for carcinogenic metals

Heavy metal	Cr	Ni	Cd	Cu	Pb	Zn	Mn
$RfD_{ing}$				4.00 × 10 <sup>-2</sup>	3.50 × 10 <sup>-3</sup>	3.00 × 10 <sup>-1</sup>	4.70 × 10 <sup>-2</sup>
$RfD_{derm}$				1.20 × 10 <sup>-2</sup>	5.25 × 10 <sup>-4</sup>	6.00 × 10 <sup>-2</sup>	2.40 × 10 <sup>-3</sup>
$RfD_{inh}$				4.02 × 10 <sup>-2</sup>	3.52 × 10 <sup>-3</sup>	3.00 × 10 <sup>-1</sup>	1.4 × 10 <sup>-5</sup>
$SF_{inh}$	42.0	0.840	6.30				

**Table 3** Statistical characteristics of the studied metal contents in soil samples

Elements	Cr	Ni	Cd	Cu	Pb	Zn	Mn	Fe
Minimum (mg/kg)	7.48	4.86	1.35	27.1	68.88	31.75	71.97	17,237.16
Maximum (mg/kg)	62.82	44.03	38.9	257.66	6762.03	1559.25	1721.9	114,033.9
Mean (mg/kg)	30.91	20.25	7.04	57.8	1093.03	867.08	358.77	34,281.45
95%ULC <sup>a</sup>	43.77	28.97	16.27	115.58	2742.43	1238.06	758.36	57,458.53
Standard deviation	16.72	11.34	12.0	75.17	2145.79	482.64	519.85	30,152.26
Variation coefficient (%)	54.09	56.00	170.45	130.05	196.32	55.66	140.90	87.96
Skewness	0.64	0.88	2.95	2.97	2.9	-0.12	2.81	2.91
Kurtosis	0.62	2.0	8.76	8.85	8.52	0.15	8.16	8.59
Chinese soil quality guideline <sup>b</sup>	300	50	0.30	100	300	250	NA	NA
The background values <sup>c</sup>	50.5	14.4	0.056	17.0	36.0	47.3	279.0	24,200.0

NA not available

<sup>a</sup> Upper limit of the 95% confidence interval for the mean

<sup>b</sup> The Grade II (pH = 6.5–7.5) of the Chinese Soil Environment Quality Standard (GB15618-1995) was chosen as the assessment standard. Grade II could be employed for the critical value to protect human health (Chinese Environmental Protection Administration (CEPA) 1995)

<sup>c</sup> The background values for the heavy metals in soils from Guangdong Province

The results revealed that the obtained concentrations varied distinctly among sampling sites. As illustrated in Table 3, the average contents of Cr, Ni, and Cu were relatively lower in paddy soils than the acceptable threshold value in the Grade II of Chinese Soil Environmental Quality standards (GB15618-1995) (CEPA 1995). When compared against their corresponding background values of soils from Guangdong province, with the exception of Cr, the mean concentrations of the other studied elements, namely, Cd, Cu, Pb, Zn, Mn, and Fe, were significantly higher; particularly, the levels of Cd, Pb, and Zn were approximately 125.71, 30.36, and 18.33 times their corresponding background values, respectively. The above observations demonstrated that the excessive concentrations, especially of Cd, Pb, and Zn, could be linked closely to the mining and smelting processes in recent decades, and thus, their potential pollutant risk should be of notable concern. Mn and Fe were also relatively higher when compared to other elements in the analyzed samples because they were major elements in most soils. Large standard deviations indicated that the studied metals of the soil samples were derived from highly heterogeneous environments or of anthropogenic origins (Leung et al. 2008). In addition, the coefficient of variation (CV) indicates the degree of spatial variability coupled generally with high concentrations of heavy metals dominated by strong anthropogenic sources (Zhao et al. 2014). For eight metals, their variation coefficients ( $CV = SD/mean \times 100$ ) followed the order  $Pb (196.32\%) > Cd (170.45\%) > Mn (140.90\%) > Cu (130.05\%) > Fe (87.96\%) > Ni (55.66\%) \approx Zn (56.00\%) > Cr (54.09\%)$ , suggesting that the variability of these measurements fell under a large concentration variation ( $CV > 36\%$ ) (Wilding 1985).

The  $CV_s$  for the studied heavy metals showed extensive variability on the small scale and were likely augmented by anthropogenic sources. Considering skewness and kurtosis, application of the Kolmogorov-Smirnov (KS) test confirmed that the concentration data only for Cr, Ni, and Zn approached a nearly normal distribution ( $P > 0.05$ ); in contrast, the other metals had strongly positive right-skewed distributions, and their values from high to low were  $Mn > Pb > Fe > Cd > Cu$ , indicating that the paddy soils were influenced by these metals to varying degrees.

#### A comparison of heavy metal concentrations in the soils studied with those of mining areas in other parts of the world

It is a common practice to further evaluate the extent of heavy metal pollution in the different mine-impacted soils. A comparison of heavy metal concentrations with those from other mining areas is summarized in Table 4. In comparison with data reported for other similar studies, the results show that the concentrations of heavy metals in the study area, apart from Pb and Fe, fell within the range of those from other regions listed. With the exception of Ghana, Cr values were lower than those recorded for the other mining areas. The average concentrations of Cd and Zn were substantially higher than those found by other investigators but lower than those provided by Liu et al. The corresponding mean contents of Ni and Mn in the present study were relatively high in comparison with other mining areas from Ghana, Slovakia, and China. Additionally, the mean Pb and Fe concentrations were

**Table 4** Comparison of the related mean values (mg kg<sup>-1</sup>) reported for other mine-impacted soils from China and other regions

Author(s)	Cr	Ni	Cd	Cu	Pb	Zn	Mn	Fe
Bempah and Ewusi. 2016 (Ghana)	16.88	41.77	0.19	16.03	19.96	61.87	445.60	531.46
Demková L et al. 2017 (Slovakia)	32.0	51.2	2.72	29.7	40.8	129	1063	23,408
Olobatoke and Mathuthu. 2017 (South Africa)	173.39	13.40	NA	17.34	17.01	49.00	42.70	NA
Liu et al. 2016 (China)	60.4	35.9	10.0	60.4	487.4	1136.1	703.7	NA
Xing et al. 2016 (China)	45.6	26.56	0.21	25.37	42.82	80.99	NA	NA
Lu et al. 2014 (China)	95.6	NA	2.3	23.5	218.6	337.8	NA	NA
Luo et al. 2016 (China)	79.37	50.63	NA	93.12	33.22	331.69	NA	NA
Zhang et al. 2014 (China)	90.24	38.60	2.86	60.46	553.67	347.36	NA	NA

NA not available

markedly higher than those measured by other previous studies. Here, it is hard to make a quantitative evaluation that the sources contaminated by various heavy metals were responsible for the differences in the concentrations. This is probably because different study areas have their specific environmental characteristics, such as anthropogenic inputs, agricultural culture modes, and topographic features.

**Contamination level evaluation of heavy metals**

The enrichment factor (EF) can be utilized to obtain primary information about the potential sources of the studied metals in the paddy soil. The EF value of each element at each site was calculated, as depicted in Fig. 2.

Following the Sutherland (2000) classification (Sutherland 2000), the order of studied metals in terms of the mean magnitude of EF levels for the classified carcinogens was Cd (extremely high pollution) > Zn (significant pollution) > Pb (significant pollution) > Cu (moderate pollution) > Ni (slight pollution) > Mn (no pollution) > Cr (no pollution). From the evaluation of EFs shown in Fig. 2, the mean EF values only of Cr (0.51) and Mn (0.72) were less than 1, indicating that they were uncontaminated. In the case of Ni, the EF values exceeded 1 but were less than 2 at all stations except for stations S3 and S7, with a mean value of 1.24, indicating a limited enrichment status. With a demonstrated mean value of 2.1, the EF values of Cu were over 1 at all locations but were over 2 and less than 5 only at sampling station S3, suggesting that Cu was relatively moderate enriched. Comparatively speaking, the EF values for the remaining metals were far more than 5, namely, Cd, Pb, and Zn, were characterized by higher EF values of 112.64, 13.79, and 16.34, respectively. According to the above findings, the EF values for Cd, Pb, and Zn were from significant to extreme, indicating the sources were predominantly from distinctive artificial activities. Undoubtedly, Cd, Pb, and Zn should be given more attention in the future.

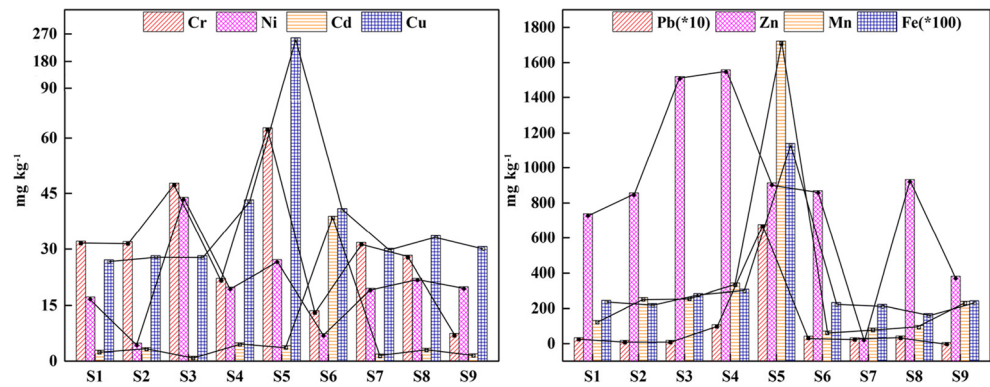
**Spatial distributions of heavy metals**

The spatial distribution trends of the studied metals in the paddy soil samples from the lead-zinc mine areas are presented in Fig. 2.

The spatial distribution trends for Cr, Cu, Pb, Mn, and Fe exhibited remarkable similarity. Additionally, relatively high concentrations were observed close to the location of the most southwestern zone of Pb-Zn mining sites and the eastern border of a small-scale smelting plant in this region. Interestingly, among nine sampling sites, maximum concentrations were found near a metalliferous site (S5). The possible reason for the distribution patterns was a similar setup in terms of sulfide mineral exploitation and nonferrous metal smelting activities. Unlike the spatial distributions of Ni and Zn, which showed an unclear relationship between their distribution trends, their variation trends of their concentrations decreased at similar sites. The variation of Cd concentrations was apparently different from that of the other metals. Soil Cd concentrations at the sampling sites followed the order S6 > S4 > S5 > S2 > S8 > S1 > S9 > S7 > S3 (Fig. 3). In particular, the highest concentration of Cd at sampling site S6 was 694.64 times greater than its corresponding background value. This observation may imply that Cd was present in residual tailings and smelting waste residue exposed to the environment and spread over the study area through water-runoff erosion and wind erosion.

The spatial distribution patterns of heavy metals may be due to the comprehensive influence of multiple factors around the mining area. Taken as a whole, the higher concentrations for most elements are readily affected by environmental factors and intensive human activities. According to our previous investigation, the predominant wind direction is southwesterly in the study area, which is surrounded by mountains in three directions (E, N, W) and whose terrain is high to the northeast and low to the southwest. In addition, the windborne transport and atmospheric deposition of fine particulates associated with mining and smelting operation emissions were controlled

**Fig. 3** Spatial distribution of the studied metal concentrations in soils



by the prevailing wind and blocked by mountains in the mining area. Therefore, it is likely that environmental factors were responsible for the trends in the spatial distributions of heavy metals. In addition, all soil samples were collected entirely from lead-zinc mine areas. Typically, high concentration distributions of heavy metals may be largely explained by extensive mining activities.

### Multivariate statistics for pollution source apportionment

Briefly, multivariate statistical analyses, including Pearson's correlation matrix, principal component analysis (PCA), and hierarchical cluster analysis (CA), were widely applied to identify the potential sources and to characterize their interactions. The relationships between the concentrations of heavy metals were investigated using Pearson's correlation coefficients, as described in Table 5. The raw data is applicable for PCA through the Kaiser-Meyer-Olkin (KMO) measure and Bartlett's sphericity test. The PCA results of the factor loadings, as well as eigenvalues, are also listed in Table 5. The spatial representation displaying the relevance of the

elements for the two rotated components is visually illustrated in Fig. 4. The CA results for the heavy metals are displayed in Fig. 5 as a hierarchical diagram.

### Correlation analysis results

Usually, significant-correlated coefficients between concentrations of heavy metals could indicate similarities in their origins. As shown in Table 5, Cu, Pb, Mn, and Fe were significantly correlated with each other ( $P < 0.01$ ), and the Pearson correlation coefficients between Cu and Pb (0.966), Cu and Mn (0.982), Cu and Fe (0.911), Pb and Mn (0.981), Pb and Fe (0.900), and Mn and Fe (0.992) were higher than 0.900. Furthermore, the correlation coefficients for the pairs Cr-Cu, Cr-Pb, Cr-Mn, and Cr-Fe were calculated to be 0.686, 0.697, 0.716, and 0.720 ( $P < 0.05$ ), respectively, which shows that Cr was significantly correlated with Cu, Pb, Mn, and Fe. The above analyses highlighted that some of the metals were probably derived from common origins. Moreover, other metal pairs exhibited weak positive correlations. For example, the correlation coefficients for Cr-Ni, Ni-Zn, and Zn-Cr were

**Table 5** Pearson correlation coefficients of the contents and principal component analysis (PCA) of the studied metals in soils

Element	Rotated matrix		Personal correlation coefficients of heavy metal concentrations							
	PC1	PC2	Cr	Ni	Cd	Cu	Pb	Zn	Mn	Fe
Component	PC1	PC2								
Cr	<b>0.69</b>	<b>0.56</b>	1	0.546	-0.377	0.686*	0.697*	0.259	0.716*	0.720*
Ni	0.16	<b>0.88</b>		1	-0.460	0.210	0.216	0.388	0.270	0.270
Cd	-0.02	-0.71			1	-0.044	-0.070	0.038	-0.167	-0.098
Cu	<b>1.00</b>	0.04				1	0.996**	0.064	0.982**	0.991**
Pb	<b>0.99</b>	0.07					1	0.104	0.981**	0.990**
Zn	0.05	<b>0.51</b>						1	0.142	0.107
Mn	<b>0.98</b>	0.15							1	0.992**
Fe	<b>0.99</b>	0.11								1
Eigenvalue	4.42	1.88								
Cumulative percent (%)	55.260	78.795								

Bold black values represent that heavy metals were strongly associated in the same factor with high loadings ( $> 0.50$ )

\*Correlation is significant at  $P < 0.05$  (two tailed);

\*\*correlation is significant at  $P < 0.01$  (two tailed)



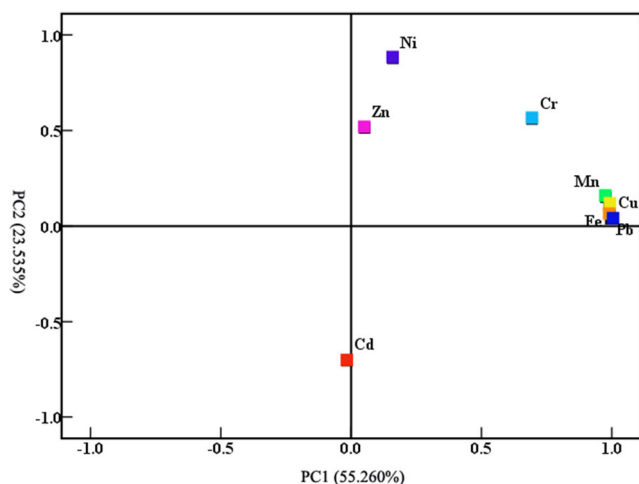


**Fig. 4** The principal component analysis rotation loading plot of the studied metals in soils

determined to be 0.546, 0.388, and 0.259. In addition, generally, negative correlation with any other metal was exhibited only for Cd, suggesting that Cd might have a completely independent behavior compared to the other elements. As mentioned earlier, Cd accumulation with a typical behavior was present at an extremely high enrichment level. This might be because Cd was inevitably discharged into the terrestrial environment through other point sources, specifically mine exploitation, metallurgy industries, and fertilizer application.

*Principal component analysis results*

The results in Table 5 and Fig. 4 indicated that the eigenvalues of the two extracted factors were greater than 1, and the two predominant factors explained 78.795% of the cumulative total variance, reflecting the comprehensive information included in the raw data. The first factor, with the higher eigenvalue

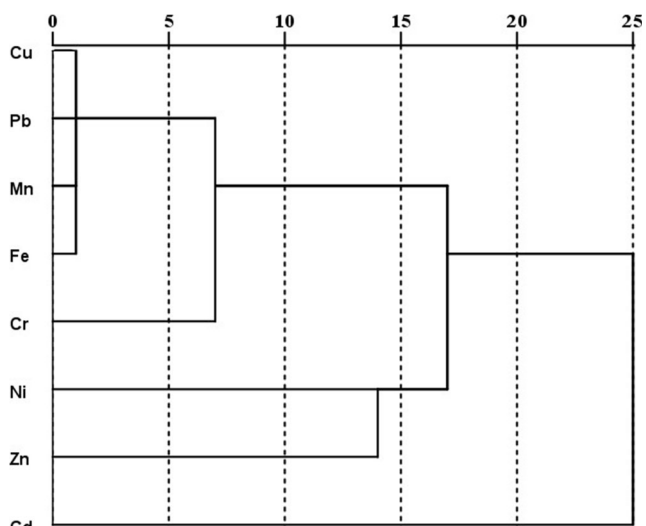


**Fig. 5** Hierarchical diagram for the studied metals in soil obtained by the cluster analysis method

value of 4.42, contributed to 55.260% of the total variance and was heavily weighted by Cr (0.69), Cu (1.00), Pb (0.99), Mn (0.98), and Fe (0.99). Historically, it can be usually inferred that Cr, Mn, and Fe might mainly be associated with high natural geological background in soils (Liang et al. 2017; Zeng et al. 2009). In more details, the concentrations of Cu, Pb, Mn, and Fe in the paddy soils were higher than their corresponding background values with high-degree variations (Table 1), among which Cu and Pb were markedly enriched elements at the small scale, whereas the concentrations of Cr were lower than its background values, with the smallest variation coefficient ( $CV > 36\%$ ). In addition, the spatial distribution trends for these elements were not only highly similar but might also have had the same source because their correlations among these elements were strong. Multiple metal ores co-occurring with Cu, Pb, Mn, and Fe can probably be extracted from sulfide minerals under acidic condition and transported over the entire area. Considering the above observations, emissions from mining operations, such as metal ore mining, smelting, and processing activities, are presumed to be the predominant component correlated to their potential to increase accumulations around the mine sites over time. Cu and Pb are anthropogenic metals usually generated by external sources. Relatively high Cu and Pb concentrations, mainly located in the high-density residential and high-traffic density area near the mining activities district, were also well documented. As a consequence, Cu could be partially ascribed to metal components of vehicles, and Pb is a well-known marker element of vehicular exhaust that might be identified as a minor source (Chen et al. 2016). Additionally, Cu and Pb were proposed to be potentially supplied from metal-containing pesticides and mineral fertilizers directly used in this region (Jiang et al. 2017; Marrugo-Negrete et al. 2017). Therefore, PC1 was controlled by the anthropogenic components related to mining industries, agricultural production, and transportation pollution occurring in the study area for lengthy periods.

In contrast, factor 2 was represented by Cr, Ni, and Zn with high loadings (loading  $> 0.50$ ) and could account for 23.535% of the total variance. In the present study, the EF results suggested that Cr and Ni were to a great extent dominated by natural origins. However, according to our previous investigation, there were indeed metal smelting and processing plants, a milk factory, and other some factories in the heavily polluted mining district. Combined with similar studies, high Cr, Ni, and Zn concentrations were often recognized as deriving from industrial sources closely associated with metal and chemical industries (Chen et al. 2016). Consequently, the industrial practices were likely another way the accumulation of Cr, Ni, and Zn was exacerbated in paddy soils. Previous studies showed that Zn and Zn compounds specifically are associated with agricultural fertilizers and animal wastes, significantly contributing to accumulation of Zn in agricultural soils (Pan et al. 2016b). Therefore, PC2 represented miscellaneous

**Table 6** Potential ecological risk coefficient ( $E_i^r$ ) and potential ecological hazard index (RI) of the studied metals in soils

Elements	$E_i^r$							RI
	Cr	Ni	Cd	Cu	Pb	Zn	Mn	
Mean	1.02	6.19	3679.26	10.51	68.96	16.34	0.72	3783.01
Minimum	0.29	1.79	476.04	7.04	9.46	0.72	0.27	683.74
Maximum	1.60	12.96	21,535.74	16.08	199.31	27.67	1.31	21,632.82

The risk indices of all heavy metals ( $RI \leq 150$ ) shows a low potential ecological hazard;  $150 \leq RI \leq 300$  shows a moderate potential ecological hazard;  $300 \leq RI \leq 600$  shows a high potential ecological hazard;  $600 \leq RI$  shows a serious potential ecological hazard

inputs associated with nearby industrial practices, agricultural activities, and natural inputs. Furthermore, Cr was represented simultaneously in PC1 and PC2 (with high loadings of 0.69 and 0.56, respectively), suggesting that Cr probably exhibited the mixed source of both lithogenic and anthropogenic activities (Yu et al. 2016).

#### Cluster analysis results

As shown in Fig. 5, the eight elements could be divided into three major groups based on the cluster analysis: (a) Cr-Cu-Pb-Mn-Fe; (b) Ni-Zn; and (c) Cd. The results were generally in accordance with those of the spatial variation characteristics, PCA, and Pearson correlation analysis.

#### Potential ecological risk assessment

The potential ecological risks for individual elements ( $E_i^r$ ) and multiple elements (RI) are summarized in Table 6, and the contributions of potential ecological risk ( $E_i^r$ ) by different heavy metals to the potential ecological risk index (RI) in soils are illustrated in Fig. 6.

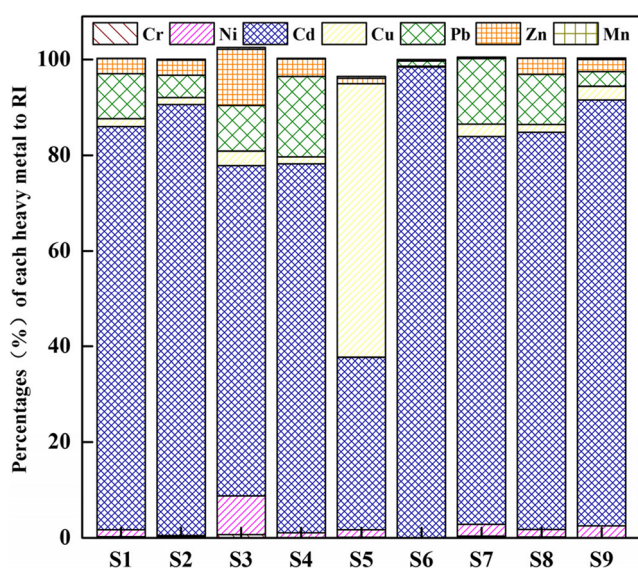


**Fig. 6** The relative contribution of potential ecological risk ( $E_i^r$ ) by each heavy metal at each station potential ecological risk index (RI) in soils

The consequences of mean  $E_i^r$  values were ranked as Cd (476.04–21,535.74) > Pb (9.46–199.31) > Zn (0.72–27.67) > Cu (7.04–16.08) > Ni (1.79–12.96) > Cr (0.29–1.60) > Mn (0.27–1.31), not entirely coinciding with the toxicity coefficients. For instance, nearly 88.9% of the samples polluted by Cd exceeded the threshold (600). By contrast, the concentrations of Cd at all stations were far smaller than those of the remaining metals in this study, whereas the extreme ecological effect of Cd was exhibited due to its very high toxic response factor. Based on the classification of Hakanson (1980), the ecological risk of the studied metals in the paddy soils ranged from low to extremely high. The  $E_i^r$  mean values of Cr, Ni, Cu, Zn, and Mn were all far below 40 at all sampling stations, indicating that these metals bore relatively low potential ecological risks and might pose only limited risks of toxicity in the study area. Moreover, the  $E_i^r$  values of Cd fluctuated across all the locations, with an  $E_i^r$  value of 3679.26. Specifically, its highest  $E_i^r$  value ( $E_i^r = 21,535.74$ ), occurring at sampling site S6, represented extremely high pollution.  $E_i^r$  values for Pb at two sampling stations (S4 and S5) showed moderate potential ecological risk ( $E_i^r = 118.42$  and 199.31). In general, 66.7% of the stations showed low or moderate ecological risk factors. From the mining perspective, there was unambiguous indication that Cd could be derived from large quantities of by-products produced by smelting/refining of Pb-Zn ores and AMD, whereas the immoderate accumulation of Pb and Zn could be contributed by the extraction process of the minerals near mine sites, such as galena (PbS) and sphalerite (ZnS) (Obiora et al. 2016).

The RI values were arranged in the sequence S6 > S8 > S4 > S2 > S1 > S7 > S9 > S3. Moreover, the RI values of each sampling site ranged from 683.74 to 21,632.82, with a mean value of 3783.1, implying that the paddy soils polluted by heavy metals at all sampling stations posed extremely high risk. As illustrated in Fig. 6, the mean contributions of  $E_i^r$  by Cr, Ni, Cd, Cu, Pb, Zn, and Mn to the RI were approximately 0.08, 0.50, 92.4, 0.76, 5.51, 1.05, and 0.06%, respectively. It was confirmed that Cd was selected as a priority pollutant because it was the main contributor to the potential ecological risk in the study area. Consequently, some measures should be undertaken on contaminated soils to reduce the adverse ecological effects.

**Table 7** Non-carcinogenic and carcinogenic risks of the studied metals in soils

Health risk	Carcinogenic risk				Non-carcinogenic risk				
	$CR_{Cr}$	$CR_{Ni}$	$CR_{Cd}$	$CR_n$	$HI_{Cu}$	$HI_{Pb}$	$HI_{Zn}$	$HI_{Mn}$	$HI_n$
Child	$5.25 \times 10^{-8}$	$6.95 \times 10^{-10}$	$2.93 \times 10^{-9}$	$5.61 \times 10^{-8}$	$3.51 \times 10^{-2}$	9.61	$5.04 \times 10^{-2}$	$2.23 \times 10^{-1}$	9.91
Adult	$1.14 \times 10^{-7}$	$1.50 \times 10^{-9}$	$6.34 \times 10^{-9}$	$1.22 \times 10^{-7}$	$2.18 \times 10^{-2}$	6.54	$3.28 \times 10^{-2}$	$2.25 \times 10^{-1}$	6.82

**Human health risk assessment**

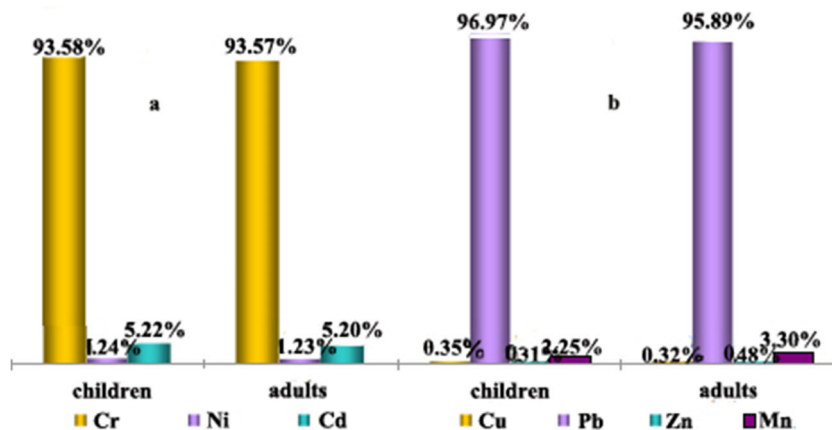
The assessment results of carcinogenic and non-carcinogenic health risks both for children and adults are presented in Table 7, and the cumulative percentage of each element for carcinogenic and non-carcinogenic effects are illustrated in Fig. 7.

For carcinogenic risk, the majority of  $CR_s$  values for carcinogenic heavy metals were between  $1.0 \times 10^{-10}$  and  $1.0 \times 10^{-7}$  and were ranked as  $CR_{Cr} > CR_{Cd} > CR_{Ni}$  both for children and adults. In addition, the  $CR_s$  posed by Cr, Ni, and Cd in soil samples for children were lower than those for adults. From the present results, it can indeed be concluded that the carcinogenic risk of exposure to Cr, Ni, and Cd is negligible in most situations, as all calculated  $CR_s$  stood in the range of internationally acceptable risk ( $1.0 \times 10^{-4}$ – $1.0 \times 10^{-6}$ ). As shown in Fig. 7a, it is very clear that the ratios of  $CR_s$  values to  $CR_n$  for children were similar to those for adults. In addition, Cr was the prominent element among the three carcinogenic elements, as it accounted for approximately 93.58 and 93.57% of the  $CR_n$  for children and adults, respectively. Therefore, the carcinogenic risk appears to be the highest for the exposure of Cr by inhalation exposure pathways, meaning that the carcinogenic risk of Cr should receive adequate attention in pollution control by the government for residential health concerns in the coming years.

Similarly, the  $HI_n$  values for children and adults were 6.82 and 9.91, respectively; the values separately greater

than 1 implied that the local inhabitants may directly suffer from potential non-carcinogenic effects in their daily life via various exposure pathways. Moreover, among the studied non-carcinogenic elements, the  $HI_s$  values for children and adults were in the sequence  $HI_{Pb} > HI_{Mn} > HI_{Zn} > HI_{Cu}$ . By comparison, the non-carcinogenic metals could cause harm to children more easily than to adults through heavy metal exposure via mine-impacted soils, indicating that children tend to be more susceptible to environmental contaminants. This might be better explained by the fact that children have more frequent hand-to-mouth behavior and higher respiration rates per unit body weight in most situations, whereby they more readily ingest quantities of contaminated soil. According to Fig. 7b, Pb was the major contributor to non-carcinogenic effects for children and adults, contributing approximately 93.58 and 93.57% of the  $HI_n$  value. By contrast, the total percentage of the other three heavy metals for the  $HI_n$  value was only 6.42% for children and 6.43% for adults. In addition, acceptable  $HI_s$  in mine-impacted soils were found for Cu, Zn, and Mn. In contrast, Pb levels were far higher than the acceptable threshold value of 1. The very high Pb exposures for local residents are most likely related to human activities such as agricultural production, vehicular emissions, and mining sources. Under these circumstances, it was apparent that the non-carcinogenic risks produced by Pb should not be overlooked, and more attention and measures should be taken to reduce the adverse health effects.

**Fig. 7** Percentage contribution of individual metals to carcinogenic and non-carcinogenic risks for children and adults



## Conclusion

The present study was undertaken to identify the pollutant characteristics and environmental risks of heavy metals in the paddy soils. Thus, the composition characteristics of the pollutant sources of the studied metals were revealed by multivariate statistical methods, and their potential ecological and human health risks were also assessed based on the PERI method and HRA model.

Based on the results in the present study, the extent of the heavy metal accumulation in paddy soils was varied. Moreover, among these metals, the most remarkable variability was detected for Pb, followed by Cd and Mn. Temporal differences in heavy metal concentration could be due to environmental factors and intensive human activities in the study area. The spatial distribution trends revealed that high concentrations of heavy metals were found near mining sites. From multivariate statistical analysis, among the present sources, it was confirmed that the dominant driving force of the emissions was longer-term mining and smelting operations. The EF and PERI revealed that Cd, Pb, and Zn were the prominent pollutants in the paddy soils and posed significantly higher potential ecological risks relative to the other heavy metals. The health risks were mainly produced by Pb, while the effect of Cr on human health was also considerable. To combat the negative consequences of mining operations, government regulators should be urged to manage these anthropogenic sources and decrease the detrimental effects from exposure to pollutants.

**Funding information** This work was supported by Guangdong Natural Science Funds for Distinguished Young Scholar (No. S2013050014122), Guangdong provincial science and technology program (No. 2014B090901040, 2015B020237003), and Guangdong Te Zhi program youth science and technology talent of project (No. 2014TQ01Z262). This is contribution No. IS-2428 from GIGCAS.

## References

- Bempah CK, Ewusi A (2016) Heavy metals contamination and human health risk assessment around Obuasi gold mine in Ghana. *Environ Monit Assess* 188(5):261–273
- CEPA (Chinese Environmental Protection Administration) (1995) Environmental quality standard for soils (GB 15618–1995), China. <http://kjs.mep.gov.cn/hjbhbz/bzwb/trhj/trhjzlbz/199603/W020070313485587994018.pdf>
- CNEMC (China National Environmental Monitoring Center) (1990) The backgrounds of soil environment in China. China Environmental Science Press, Beijing (in Chinese)
- Chen T, Chang Q, Liu J, Clevers JG, Kooistra L (2016) Identification of soil heavy metal sources and improvement in spatial mapping based on soil spectral information: a case study in northwest China. *Sci Total Environ* 565:155–164
- Dehghani S, Moore F, Keshavarzi B, Hale BA (2016) Health risk implications of potentially toxic metals in street dust and surface soil of Tehran, Iran. *Ecotox Environ Safe* 136:92–103
- Demková L, Árvay J, Bobuľská L, Tomáš J, Stanovič R, Lošák T, Harangozo L, Vollmannová A, Bystrická J, Ján Jobbágy JM (2017) Accumulation and environmental risk assessment of heavy metals in soil and plants of four different ecosystems in a former polymetallic ores mining and smelting area (Slovakia). *J Environ Sci Health A* 1–12
- Diami SM, Kusin FM, Madzin Z (2016) Potential ecological and human health risks of heavy metals in surface soils associated with iron ore mining in Pahang, Malaysia. *Environ Sci Pollut Res* 23:1–12
- Fernandez-Calvi D, Cutillas-Barreiro L, Paradelo-Núñez R, Nóvoa-Muñoz JC, Fernandez-Sanjurjo MJ, Alvarez-Rodríguez E, Núñez-Delgado A, Arias-Estevéz M (2017) Heavy metals fractionation and desorption in pine bark amended mine soils. *J Environ Manage* 192: 79–88
- Ferreira-Baptista L, Miguel ED (2005) Geochemistry and risk assessment of street dust in Luanda, Angola: a tropical urban environment. *Atmos Environ* 39:4501–4512
- Gąsiorek M, Kowalska J, Mazurek R, Pająk M (2017) Comprehensive assessment of heavy metal pollution in topsoil of historical urban park on an example of the Planty Park in Krakow (Poland). *Chemosphere* 179:148–158
- Hakanson L (1980) An ecological risk index for aquatic pollution control—a sedimentological approach. *Water Res* 14:975–1001
- Jiang Y, Chao S, Liu J, Yang Y, Chen Y, Zhang A, Cao H (2017) Source apportionment and health risk assessment of heavy metals in soil for a township in Jiangsu Province, China. *Chemosphere* 168:1658–1668
- Kpan JDA, Opoku BK, Gloria A (2014) Heavy metal pollution in soil and water in some selected towns in Dunkwa-on-Offin district in the central region of Ghana as a result of small scale gold mining. *J Agr Chem Environ* 03:40–47
- Lei K, Giubilato E, Critto A, Pan H, Lin C (2016) Contamination and human health risk of lead in soils around lead/zinc smelting areas in China. *Environ Sci Pollut Res* 23:13128–13136
- Leung AO, Duzgorenaydin NS, Cheung KC, Wong MH (2008) Heavy metals concentrations of surface dust from e-waste recycling and its human health implications in southeast China. *Environ Sci Technol* 42:2674–2680
- Li ZY, Ma ZW, van der Kuijp TJ, Yuan ZW, Huang L (2014) A review of soil heavy metal pollution from mines in China: pollution and health risk assessment. *Sci Total Environ* s468–469:843–853
- Liang J, Feng C, Zeng G, Gao X, Zhong M, Li X, He X, Fang Y (2017) Spatial distribution and source identification of heavy metals in surface soils in a typical coal mine city, Lianyuan, China. *Environ Pollut* 225:681–690
- Liao J, Ru X, Xie B, Zhang W, Wu H, Wu C, Wei C (2017) Multi-phase distribution and comprehensive ecological risk assessment of heavy metal pollutants in a river affected by acid mine drainage. *Ecotox Environ Safe* 141:75–84
- Liao J, Wen Z, Ru X, Chen J, Wu H, Wei C (2016) Distribution and migration of heavy metals in soil and crops affected by acid mine drainage: public health implications in Guangdong Province, China. *Ecotox Environ Safe* 124:460–469
- Lin M, Gui H, Wang Y, Peng W (2017) Pollution characteristics, source apportionment, and health risk of heavy metals in street dust of Suzhou, China. *Environ Sci Pollut Res* 24(2):1987–1998
- Liu G, Wang J, Zhang E, Jing H, Liu X (2016) Heavy metal speciation and risk assessment in dry land and paddy soils near mining areas at Southern China. *Environ Sci Pollut Res* 23:8709–8720
- Lu SJ, Wang YY, He L (2014) Heavy metal pollution and ecological risk assessment of the paddy soils around a Pb-Zn mine in Huize Country. *Ecotox Environ Sci* 23(11):1832–1838 (in Chinese)
- Luo L, Liu MX, Dong FQ, Xiang F, Zhang GG, Zong MR (2016) Speciation distribution characteristics of heavy metals in soil of multi-metal mining pastoral area and pollution assessment. *J Agro-Environ Sci* 35(8):1523–1531 (in Chinese)

- Marrugo-Negrete J, Pinedo-Hernández J, Díez S (2017) Assessment of heavy metal pollution, spatial distribution and origin in agricultural soils along the Sinú River Basin, Colombia. *Environ Res* 154:380–388
- MEPPRC (Ministry of Environmental protection of the Peoples' Republic of China) (2014) HJ 25.3-2014 Technical guidelines for risk assessment of contaminated sites, China (in Chinese)
- Obiora SC, Chukwu A, Davies TC (2016) Heavy metals and health risk assessment of arable soils and food crops around Pb–Zn mining localities in Enyigba, southeastern Nigeria. *J Afr Earth Sci* 116: 182–189
- Olobatoke RY, Mathuthu M (2016) Heavy metal concentration in soil in the tailing dam vicinity of an old gold mine in Johannesburg, South Africa. *Canadian J Soil Sci* 96(3):299–304
- Olobatoke RY, Mathuthu M (2017) Heavy metal concentration in soil in the tailing dam vicinity of an old gold mine in Johannesburg, South Africa. *Canadian J Soil Sci* 96(3):299–304
- Pan L, Ma J, Hu Y, Su B, Fang G, Wang Y, Wang Z, Wang L, Xiang B (2016a) Assessments of levels, potential ecological risk, and human health risk of heavy metals in the soils from a typical county in Shanxi Province, China. *Environ Sci Pollut Res* 23:19330–19340
- Pan LB, Ma J, Wang XL, Hou H (2016b) Heavy metals in soils from a typical county in Shanxi Province, China: levels, sources and spatial distribution. *Chemosphere* 148:248–254
- Rajae M, Long RN, Renne EP, Basu N (2015) Mercury exposure assessment and spatial distribution in a Ghanaian small-scale gold mining community. *Int J Environ Res Pub Health* 12(9):10755–10782
- Ran X, Shuang W, Li R, Wang JJ, Zhang Z (2017) Soil heavy metal contamination and health risks associated with artisanal gold mining in Tongguan, Shaanxi, China. *Ecotox Environ Safe* 141:17–24
- RAIS (Risk Assessment Information System) (2014) US Department of Energy's OROO. US Department of Energy's, Oak Ridge Operations Office
- Sutherland RA (2000) Bed sediment-associated trace metals in an urban stream, Oahu, Hawaii. *Environ Geol* 39:611–627
- Ungureanu T, Iancu GO, Pintilei M, Chicoş MM (2016) Spatial distribution and geochemistry of heavy metals in soils: a case study from the NE area of Vaslui county, Romania. *J Geochem Explor* 176:20–32
- US EPA (United States Environment Protection Agency) (1989) Risk assessment guidance for superfund, volI: human health evaluation manual. EPA/540/1–89/002. Office of Solid Waste and Emergency Response, Washington
- US EPA (United States Environment Protection Agency) (2002) Supplemental guidance for developing soil screening levels for superfund sites. OSWER9355. Office of Solid Waste and Emergency Response, Washington, pp 4–24
- Wilding LP (1985) Spatial variability: its documentation, accommodation and implication to soil survey. *Spat Var* 166–193
- Wu J, Song J, Li W, Zheng M (2016) The accumulation of heavy metals in agricultural land and the associated potential ecological risks in Shenzhen, China. *Environ Sci Pollut Res* 23:1428–1440
- Xiao Q, Zong Y, Lu S (2015) Assessment of heavy metal pollution and human health risk in urban soils of steel industrial city (Anshan), Liaoning, Northeast China. *Ecotox Environ Safe* 120:377–385
- Xing YX, Yan GX, Hou QL, SUN N, Pan XT (2016) Spatial distribution and pollution characteristics of heavy metals in soil of Mentougou mining area of Beijing City, China. *J Agric Resour Environ* 33(5): 499–507 (in Chinese)
- Yu L, Cheng J, Zhan J, Jiang A (2016) Environmental quality and sources of heavy metals in the topsoil based on multivariate statistical analyses: a case study in Laiwu City, Shandong Province, China. *Nat Hazards* 81:1–11
- Zeng G, Liang J, Guo S, Shi L, Xiang L, Li X, Du C (2009) Spatial analysis of human health risk associated with ingesting manganese in Huangxing Town, Middle China. *Chemosphere* 77:368–375
- Zhang AX, Nie YN, Ji HB, Feng JG, Qin F (2014) Spatial distribution, fractionation and pollution assessment of heavy metals in Wanzhuang gold mining field in upstream part of water conservation area of Beijing, China. *J Agro-Environ Sci* 33(12):2321–2328 (in Chinese)
- Zhang C, Nie S, Liang J, Zeng G, Wu H, Hua S, Liu J, Yuan Y, Xiao H, Deng L, Xiang H (2016) Effects of heavy metals and soil physico-chemical properties on wetland soil microbial biomass and bacterial community structure. *Sci Total Environ* 557–558:785–790
- Zhao L, Xu Y, Hou H, Shangguan YX, Li F (2014) Source identification and health risk assessment of metals in urban soils around the Tangu chemical industrial district, Tianjin, China. *Sci Total Environ* 468–469:654–662